Enhanced lattice-displacement effects on the crystal field and the anomalous magnetic anisotropy in cerium monopnictides

Robert Siemann and Bernard R. Cooper
Department of Physics, West Virginia University, Morgantown, West Virginia 26506
(Received 16 June 1978)

Extremely strong ⟨100⟩ magnetic anisotropy occurs in CeSb and CeBi. This contrasts with the theoretical crystal-field-only ⟨111⟩ easy direction as found experimentally upon diluting the Ce with Y or La. We find that the strong ⟨100⟩ anisotropy can be understood when one includes elastic and magnetoelastic effects in conjunction with magnetic ordering. Depending on the system parameter values, there are two possible types of magnetic anisotropy and distortional behavior: either (i) a small expansive trigonal distortion and magnetic ordering along ⟨111⟩, or (ii) tetragonal distortion, above a significant threshold value at 0 °K, and ordering along ⟨100⟩. For the tetragonal distortion, the c/a ratio is <1 as found experimentally in CeBi. Our self-consistent calculations for CeBi use the experimental crystal-field splitting, T_N, and elastic constants. The occurrence of the tetragonally distorted ⟨100⟩ phase is associated with the remarkable sensitivity of the crystal-field interaction to lattice spacing in the cerium monopnictides. We introduce this effect via a charge-enhancement factor ρ multiplying the point-charge-model result for distortional crystal-field terms. The Γ_7 crystal-field ground state has no quadrupole moment. Because of this, distortional effects of any significance occur only with a molecular field present, as in our model calculation for CeBi, or in the absence of exchange, for ρ above a threshold value necessary to give sufficiently strong $\Gamma_7 - \Gamma_8$ mixing.

I. INTRODUCTION

Cerium bismuthide[1–6] and cerium antimonide[3,6–14] display extraordinary magnetic behavior through their highly anisotropic and unusual magnetic-ordering structures.[15] A central feature of this anomalous behavior is the presence and strength of magnetic anisotropy favoring the alignment of the magnetically ordered moments along ⟨100⟩ despite the fact that the crystal field favors a ⟨111⟩ easy axis.[3,9,10] The question then arises, is there one fundamental physical property that governs the unusual magnetic phenomenology observed?

The interest in this question is enhanced by the striking similarity[16] between the unusual magnetic properties of the cerium monopnictides with NaCl structure and the light actinide monopnictides also with NaCl structure, which show similarly strong and anomalous ⟨100⟩ magnetic ordering as well as similar and unusual highly anisotropic linear-magnetic structures. The common feature of these two classes of materials is that in both cases the f electrons responsible for the magnetic behavior ($4f$ for cerium and $5f$ for the actinides) are relatively loosely bound, say compared to $4f$ electrons in the heavy rare earths, and therefore, are much more sensitive to interactions with the crystalline lattice. Indeed from neutron scattering work and other measurements we know that the crystal field for the cerium monopnictides differs from that of the heavier rare-earth monopnictides in having a variation with lattice parameter extraordinarily stronger than that expected on the basis of the point-charge model.[17]

The main point of this paper[18] is to show that, in fact, the extraordinarily strong ⟨100⟩ anisotropy and associated properties in CeBi follow as a direct consequence of the extreme sensitivity of the crystal field to lattice displacement. Inferentially, we believe that this is also true for CeSb and the light actinide monopnictides. Besides discussing CeBi specifically, we discuss general features of magnetic-ordering phenomenology and of lattice-distortional behavior to be expected on the basis of the physical effects included in our model. Our calculations demonstrate that the ⟨100⟩ orientation of magnetic ordering with associated tetragonal compression is favored over the alternative of ⟨111⟩ ordering with trigonal expansion because of overall-energy-balance considerations involving both crystal-field and elastic energies.[19] The ⟨100⟩ tetragonal state is relatively less favorable than the ⟨111⟩ trigonal state from the point of view of crystal-field energy; but, on the other hand, the ⟨100⟩ tetragonal state is relatively less unfavorable from the point of view of the elastic energy, and the latter effect leads to the ⟨100⟩ tetragonal state winning out in the overall energy balance.

In Sec. II we discuss some details of the experimental background of interest and the physical

phenomena involved in our model calculations. The way in which the physical phenomena are represented through use of a model Hamiltonian is discussed in Sec. III; while the results of our calculations with that model Hamiltonian and their relevance to the experimental behavior are discussed in Sec. IV.

II. EXPERIMENTAL BACKGROUND AND PHYSICAL PHENOMENA INVOLVED

CeBi has NaCl crystal structure with a lattice constant[6] of 6.49 Å. The Ce^{3+} free-ion ground-state multiplet is $^2F_{5/2}$. A cubic crystal field splits the free-ion multiplet into a Γ_7 doublet and a Γ_8 quartet. For CeBi, the Γ_8 quartet is 10 °K above the Γ_7 doublet.[17,20] Type-I antiferromagnetic ordering occurs in CeBi at[2] $T_N = 25$ °K with a second-order transition. There is a first-order transition to a type-IA magnetic structure at[2] a temperature of approximately $\frac{1}{2}T_N$. A tetragonal distortion[6] with $c/a < 1$, i.e., compressive, appears in coincidence with the second-order transition and at 0 °K has grown to a value with $c/a - 1 \simeq -1 \times 10^{-3}$. For CeSb the magnetic behavior is more involved[12–14] than that of CeBi, with a series[3] of six magnetic structures with varying temperature, separated by first-order magnetic transitions. Again, however, the direction of magnetic ordering is ⟨100⟩ and there is a tetragonal distortion with $c/a < 1$ growing to $c/a - 1 \simeq -1 \times 10^{-3}$ at $T = 0$. Thus both CeBi and CeSb display ⟨100⟩ easy axes of magnetization despite the prediction[9] of a ⟨111⟩ easy axis for crystal-field-only anisotropy. For both materials, on diluting the Ce with Y, La, or a combination of the two, there is a change[3,9] from a ⟨100⟩ to a ⟨111⟩ easy direction as expected for crystal-field-only anisotropy. This experimental behavior in CeBi and CeSb suggests that a cooperative interaction besides the exchange field exists between the Ce atoms, and that this interaction may occur via magnetoelastic effects. We also note that for both (Ref. 2) CeBi and (Ref. 13) CeSb the magnetization remains close to saturation for a wide range of temperature on increasing temperature from $T = 0$.

Our present work, as reported in this paper, focuses on the occurrence of the strong ⟨100⟩ anisotropy and how this may be understood through magnetoelastic effects. We consider in detail the association between the easy direction of magnetization and the nature of crystal-lattice distortional behavior. We consider the possible crystal-lattice distortional behavior both in the presence of magnetic ordering and in its absence. For purposes of comparison to experimental behavior in the magnetic-ordering case, we consider the behavior of CeBi; where, however, for the present discussion we disregard the transition to a IA magnetic structure with decreasing temperature. We will discuss the possible relationship of the occurrence of the IA magnetic structure to more involved lattice structure behavior[19] in a future paper.

We find that the observed magnetic anisotropy and lattice distortional behavior of CeBi, as well as a quite flat sublattice magnetization variation with temperature at low T, can be understood on the basis of a simple model which includes crystal-field, elastic, and exchange effects. The central feature of this model is the enhancement of the change in crystal-field interaction with lattice displacement relative to that expected on the basis of the point-charge model. As discussed in Ref. 17 and shown in Table I, the crystal-field behavior of the cerium monopnictides deviates markedly from the $1/a^5$ dependence expected from the point-charge model. The changes in crystal-field splitting between CeBi and any of the other three compounds is about a factor of 30 times that expected from the point-charge model; while that between CeSb and the heavier compounds is about a factor of 8 or 9 larger than expected. (For CeBi, the value of Δ_{CF}, the $\Gamma_7 - \Gamma_8$ cubic-crystal-field splitting, shown in Table I is that of Ref. 20. In Ref. 17 a value about half as large was found, leading then to about twice the enhancement factors stated above.) The cerium monopnictides are unique among the rare-earth monopnictides in showing such an effect. This effect serves as the physical basis for the enhancement factor ρ, we will introduce subsequently, increasing the change in crystal-field value with lattice displacement from that expected for the point-charge model.

We will show that for enhancement of crystal-field effects associated with distortions beyond a threshold value, consistent in magnitude with the considerations just discussed, ⟨100⟩ becomes the easy direction of magnetic ordering. In doing this, we will

TABLE I. Values for Néel temperature (T_N), crystal-field splitting (Δ_{CF}), and lattice parameter (a) for the cerium monopnictides. References are given below.

	T_N (°K)	Δ_{CF} (°K)	a (Å)
CeP	9.0[a]	172[c]	5.93[f]
CeAs	7.5[a]	140[d]	6.04[f]
CeSb	16[a]	38[e]	6.39[f]
CeBi	25[b]	10[e]	6.49[g]

[a]Reference 8 and 13.
[b]Reference 2.
[c]Reference 21.
[d]Reference 22.
[e]Reference 20.
[f]Reference 23.
[g]Reference 6.

show that the fact that the size of crystal-field enhancement has a threshold to have ⟨100⟩ ordering implies that there is a corresponding threshold for the size of ⟨100⟩ compressional distortion, beyond which there is a ⟨100⟩ easy direction of magnetic anisotropy. The existence of this distortion and the associated changes in the states of the Ce^{3+} ions may be regarded as equivalent in effect to a quadrupole coupling between the Ce^{3+} ions. The quadrupolar interaction aids the exchange interaction in maintaining a large magnetic moment at low temperatures, as observed[2] by the "flat" sublattice magnetization curve at low temperature. In fact our calculations predict a contractive ⟨100⟩ distortion in agreement with experiment; and our calculations show that a contractive ⟨100⟩ distortion tends to increase the moment (i.e., keeps it from decreasing as rapidly with temperature as it would in the absence of distortion), while an expansion distortion would tend to decrease the moment.

III. MODEL HAMILTONIAN

A. Crystal field

The crystal-field Hamiltonian has the form[24]

$$\mathcal{H}_{\rm CF}=\sum_{n,m}A_{nm}O_n^m \ , \tag{3.1}$$

where the O_n^m are the Stevens[25] operator equivalents which act on the free-ion ground-state multiplet. The site symmetry and direction of quantization determine which operators are present.

For the undistorted (cubic) crystal with the ⟨100⟩ crystal direction chosen as the z axis, we have

$$\mathcal{H}_{\rm CF}=\mathcal{H}_0^{100}\equiv B_4(O_4^0+5O_4^4) \ . \tag{3.2}$$

If the ⟨111⟩ direction is taken as the polar axis, then we have

$$\mathcal{H}_{\rm CF}=\mathcal{H}_0^{111}\equiv -\tfrac{2}{3}B_4(O_4^0-20(2)^{1/2}O_4^3) \ . \tag{3.3}$$

For positive B_4 the Γ_7 state is below the Γ_8. In the point-charge model the splitting $\Delta_{\rm CF}$ between these two states is given by[24]

$$\tfrac{1}{360}\Delta_{\rm CF}\equiv B_4=\tfrac{7}{16}(Ze^2/d^5)\beta_J\langle r^4\rangle \ , \tag{3.4}$$

where β_J is the Stevens[25] multiplicative factor, d is the nearest-neighbor anion-cation distance, and $\langle r^4\rangle$ is a radial integral as calculated by Freeman and Watson,[26] and where we have taken the crystal field as corresponding to point charges on the nearest-neighbor anions. Fitting this expression to the measured crystal-field splitting of 10 °K, we then determine the effective charge Ze (e is the electron charge) on the neighboring anions.

We treat small distortions from the cubic structure by including terms in the crystal field up to second order in the anion displacements. This introduces additional crystal-field operators. For a ⟨100⟩ (tetragonal) distortion we then have

$$\mathcal{H}_{\rm CF}=\mathcal{H}_0^{100}+C_{20}O_2^0+C_{40}O_4^0 \ , \tag{3.5}$$

where

$$C_{20}=x\rho\Delta_{\rm CF}(\tfrac{1}{360}\delta-\tfrac{1}{180}\delta^2) \ , \tag{3.6}$$

$$C_{40}=\rho\Delta_{\rm CF}(\tfrac{1}{126}\delta+\tfrac{1}{42}\delta^2) \ . \tag{3.7}$$

In these expressions, Δ_{CF} is the cubic-crystal-field splitting between the Γ_7 and Γ_8 states, ρ is an enhancement factor shortly to be discussed, δ is the fractional displacement of the anions from the cubic positions, $\delta=(c-a)/a$, and the quantity x is given by

$$x\equiv -\tfrac{48}{7}(\alpha_J/\beta_J)(\langle r^2\rangle/\langle r^4\rangle)\,d^2 \ , \tag{3.8}$$

where α_J is a Stevens[25] multiplicative factor and again we use the values of the radial integrals $\langle r^2\rangle$ and $\langle r^4\rangle$ as determined by Freeman and Watson.[26] Numerically x is of the order of 10^3, making the quadrupole O_2^0 term in Eq. (3.5) the dominant distortion term.

As already discussed, the crystal-field interaction for the cerium monopnictides is extremely sensitive to the lattice displacements. If this enhancement of the effect of lattice displacements, relative to that expected for the point-charge model did not occur, then the coefficients for the distortion terms, given in Eqs. (3.6) and (3.7), would be completely determined by the measured crystal-field splitting and the size of the distortion. We represent this sensitivity in the simplest possible way by introducing an enhancement factor ρ, which increases the effect of the distortion terms in the Hamiltonian. From Eq. (3.4) we see that this is equivalent to assuming an enhancement with distortion of the effective charge and for this reason we refer to ρ as the crystal-field gradient charge-enhancement factor. The effect of the distortion on the crystal field is increased relative to the effect in the point-charge model if $\rho>1$, is decreased if $\rho<1$, and is unchanged if $\rho=1$. In our simple model we take ρ to be a fixed number that does not vary with the size of the distortion. This is, of course, a crude parametrization for what is undoubtedly a very complex effect. The variation between the pure compounds as shown in Table I, each having cubic symmetry with a different lattice parameter, certainly provides strong evidence of the sensitivity of the crystal field to lattice displacement. Obviously for small displacements about the undistorted configuration for each compound, the enhancement, relative to the point-charge model of the crystal-field

change, or the lack thereof, may very well be quite different for displacements, i.e., distortions, of a differing nature. In this regard, experiments measuring the change in crystal-field splitting under hydrostatic pressure and uniaxial stress would be very valuable.

For a ⟨111⟩ (trigonal) distortion, the corresponding effect of distortion on the crystal field is given by

$$\mathcal{H}_{CF} = \mathcal{H}_0^{111} + C_{20}O_2^0 + C_{40}O_4^0 + C_{43}O_4^3 \ , \quad (3.9)$$

where

$$C_{20} = -x\rho\Delta_{CF}(\delta/180(3)^{1/2} - 7\delta^2/1080) \ , \quad (3.10)$$

$$C_{40} = \rho\Delta_{CF}(\delta/252(3)^{1/2} + \delta^2/63) \ , \quad (3.11)$$

$$C_{43} = \rho\Delta_{CF}([-2(6)^{1/2}/27]\delta + [(2)^{1/2}/9]\delta^2) \ . \quad (3.12)$$

Here δ is the relative change in the ⟨111⟩ component of the nearest-neighbor cation-anion distance. The quadrupole term is also dominant for the ⟨111⟩ distortion.

B. Exchange interaction

We treat the exchange interaction in the molecular-field approximation as in Wang and Cooper.[27] The Heisenberg interaction is then replaced by the single-site Hamiltonian

$$\mathcal{H}_{MF} = -\lambda\langle J_z\rangle J_z + \tfrac{1}{2}\lambda\langle J_z\rangle^2 \ , \quad (3.13)$$

where the brackets denote a thermal average. We assume that this interaction is isotropic so that the exchange constant λ has the same value whether the magnetic ordering occurs along the ⟨100⟩ or ⟨111⟩ direction. The value of λ is selected so that the Néel temperature of the model (including crystal field and elastic effects) corresponds to the experimental value of 25 °K for CeBi.

C. Elastic energy

To determine the elastic energy we adopt a microscopic central-force model[28] with nearest-neighbor force constants k_{aa}, k_{cc}, and k_{ac} between anion-anion, cation-cation, and anion-cation pairs, respectively. For the tetragonal distortion the elastic energy per Ce^{3+} ion is given by

$$\mathcal{H}_{EL} = (k_{aa} + k_{cc} + k_{ac})\delta^2 \ . \quad (3.14)$$

For the trigonal distortion we have

$$\mathcal{H}_{EL} = 4(k_{aa} + k_{cc} + \tfrac{1}{4}k_{ac})\delta^2 \ . \quad (3.15)$$

Two different macroscopic-elastic constants have been measured[29] for CeBi. To determine the two combinations of microscopic constants that occur in Eqs. (3.15) and (3.16), $k_{aa}+k_{cc}$ and k_{ac}, we fit the measured macroscopic values.

D. Eigenvalues and eigenfunctions, charge-cloud shape.

The total Hamiltonian for a single Ce^{3+} ion then becomes

$$\mathcal{H} = \mathcal{H}_{CF} + \mathcal{H}_{MF} + \mathcal{H}_{EL} \ . \quad (3.16)$$

We have calculated the eigenvalues of $\mathcal{H}_{CF} + \mathcal{H}_{MF}$, neglecting the overall additive constant given by the second term of $\mathcal{H}_{MF}$ in Eq. (3.13). This has been done for distortion and magnetic ordering along ⟨100⟩ as shown in Fig. 1, and along ⟨111⟩ as shown in Fig. 2. We have also determined the corresponding eigenfunctions.

We shall frequently refer to the shape of the electronic charge cloud for an eigenstate. This shape may be determined by using the position representation of the multiplet states, which for the ground-state multiplet of Ce^{3+} is given by

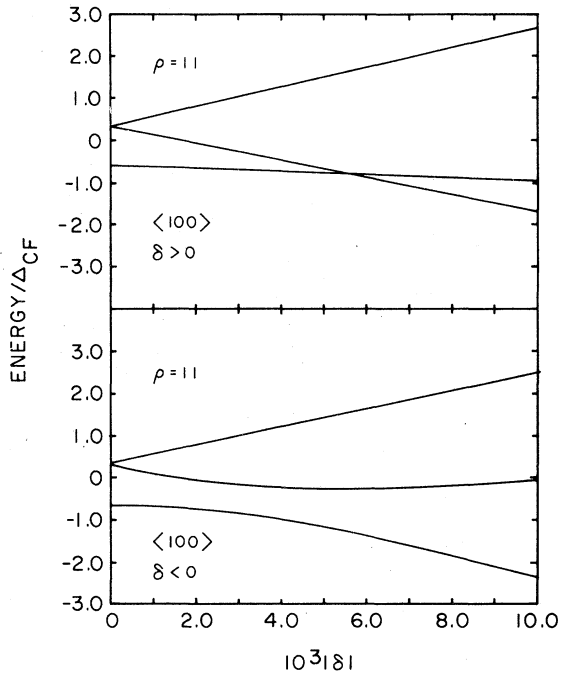

FIG. 1. Variation of the crystal-field energy levels with tetragonal distortion in the absence of magnetic ordering and with a crystal-field distortion enhancement factor ρ of 11. The energies are scaled to the cubic-crystal-field splitting Δ_{CF}, and the value for CeBi has been used for the nearest-neighbor anion-cation distance. Upper panel is for expansive distortion; lower panel is for compressive distortion.

$$\langle\theta,\phi|J_z\rangle=(2l+1)^{-1/2}[-(l-J_z+\tfrac{1}{2})\,Y_{l,J_z-1/2}(\theta,\phi)\chi_+ +(l+J_z+\tfrac{1}{2})\,Y_{l,J_z+1/2}(\theta,\phi)\chi_-] \ , \tag{3.17}$$

with $l=3$. $Y_{lm}(\theta,\phi)$ is a spherical harmonic, and $\chi_\pm$ are spin-$\frac{1}{2}$ spinors. So that the charge-cloud shape as a function of θ and ϕ for the state with $J=\frac{5}{2}$ and specified J_z is given by

$$\Omega_{J,J_z}(\theta,\phi)=[(l-J_z+\tfrac{1}{2})/(2l+1)]\,|Y_{l,J_z-1/2}|^2+[(l+J_z+\tfrac{1}{2})/(2l+1)]\,|Y_{l,J_z+1/2}|^2 \ . \tag{3.18}$$

IV. BEHAVIOR OF THE MODEL AND COMPARISON WITH BEHAVIOR IN CeBi

A. Free energy

The free energy of the system is given by

$$G(\beta,\langle J_z\rangle,\delta)=-kT\ln\left(\sum_i\exp(-\beta E_i)\right)+\tfrac{1}{2}\lambda\langle J_z\rangle^2+\mathcal{H}_{\rm EL} \ , \tag{4.1}$$

with the E_i given by Eqs. (3.18) – (3.21), and where T is the temperature, k is Boltzmann's constant, and $\beta=1/kT$.

The equilibrium values of the magnetization $\langle J_z\rangle$, and the distortion δ, are found by minimizing the free energy with respect to both variables. The first minimization condition

$$\frac{\partial G}{\partial\langle J_z\rangle}=0 \tag{4.2}$$

leads to the usual molecular field self-consistency requirement that the molecular field parameter $\langle J_z\rangle$ in the Hamiltonian be the same as the thermal average of J_z. A nonzero value of $\langle J_z\rangle$ implies the presence of magnetic ordering.

Applying the second minimization condition

$$\frac{\partial G}{\partial\delta}=\frac{\partial}{\partial\delta}[-kT\,\mathrm{lnTr}(e^{-\beta\mathcal{H}})+\mathcal{H}_{\rm EL}]=0 \ , \tag{4.3}$$

we see that the distortion may be expressed in terms of the thermal average of an appropriate combination of multipole operators. If we consider only the dominant quadrupole term in the Hamiltonian of Eq. (3.5) or (3.9) to first order in δ, then Eq. (4.3) becomes

$$\delta=-Q\langle O_2^0\rangle \ , \tag{4.4}$$

and the crystal field and elastic Hamiltonian becomes

$$\mathcal{H}=\mathcal{H}_0-Q\langle O_2^0\rangle O_2^0+\tfrac{1}{2}Q\langle O_2^0\rangle^2 \ , \tag{4.5}$$

where, as previously introduced, $\mathcal{H}_0$ is the crystal-field Hamiltonian in the absence of distortion, and where, for a $\langle 100\rangle$ distortion,

$$Q=\tfrac{1}{2}(\tfrac{1}{360}x\rho\Delta_{\rm CF})^2(k_{aa}+k_{cc}+k_{ac})^{-1} \ . \tag{4.6}$$

Eq. (3.5) has exactly the same form as the molecular-field Hamiltonian of Eq. (3.14). A nonzero value of $\langle O_2^0\rangle$ implies the existence of a quadrupolar ordering. Allowing for a distortion of the lattice introduces an effective quadrupolar coupling[30] between the Ce^{3+} ions. The strength of this coupling, from Eq. (4.6), is proportional to the charge enhancement and inversely proportional to the size of the elastic constants. We thus have two types of ordering occurring in the model.

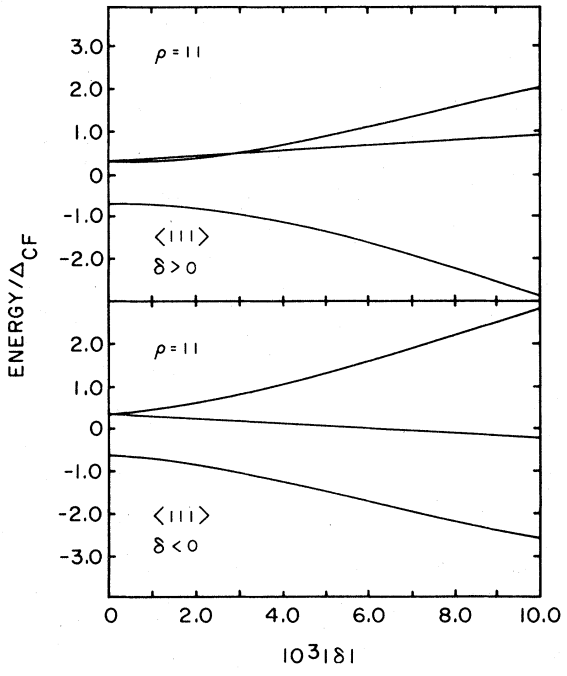

FIG. 2. Variation of the crystal-field energy levels with trigonal distortion in the absence of magnetic ordering. Parameters are as in Fig. 1. Upper panel is for expansive distortion; lower panel is for compressive distortion.

B. No magnetic ordering

We first consider the behavior for the model with no magnetic ordering, so that $\langle J_z\rangle=0$. The essential aspects can be seen by considering the $T=0$ behavior which depends solely on the ground-state properties. The cubic Γ_7 ground state is rather insensitive to lattice displacements along either the $\langle 100\rangle$ or $\langle 111\rangle$

directions. This can be seen from the first-order perturbative corrections to the Γ_7 state given by Eq. (3.20a) or Eq. (3.21a). Only the less important octupole terms in the Hamiltonian yield a first-order correction. This is because the Γ_7 electronic charge cloud consists of 12 lobes arranged in cubic symmetry, and hence, possesses no quadrupole moment. The distortion effects are therefore, minimal. However, a lattice distortion produces strong mixing between the Γ_7 and Γ_8 states, and for sufficiently large displacements the ground state acquires a large quadrupole moment. (Alternatively the quadrupole effect within the Γ_8 states may cause one pair of those states to drop enough in energy for a distortion of sufficient size to give a level crossing and a new ground state possessing a well-defined quadrupole moment.) The crystal-field energy then decreases linearly with further distortion. This decrease may be able to balance the increase in elastic energy, and an equilibrium distortion may result. We can consider these distortion effects on the crystal-field behavior in detail by examining the effects of various types of distortion on the energy-level behavior. This is shown for $\langle 100 \rangle$ (tetragonal) distortions in Fig. 1 and for $\langle 111 \rangle$ (trigonal) distortions in Fig. 2. We take a crystal-field charge enhancement factor ρ of 11 and the nearest-neighbor anion-cation distance as that of CeBi.

For the $\langle 100 \rangle$ distortions, we first consider a positive displacement ($\delta > 0$). For small distortions the ground-state energy remains essentially unchanged. The distortion splits the Γ_8 quartet into pairs, and each individual state has a large quadrupole moment as evidenced by the linear variation of energy shown for these states in Fig. 1. The pair of states $|\pm\frac{1}{2}\rangle$ lowers its energy with the distortion. These states remain pure and do not mix with the Γ_7 states. At $\delta \simeq 5.5 \times 10^{-3}$ the $|\pm\frac{1}{2}\rangle$ state crosses the Γ_7 level and becomes the new ground state. Further distortion lowers the crystal-field ground-state energy.

The approximate location of this level crossing for the $\langle 100 \rangle$ case with $\delta > 0$ may be determined from first-order perturbation theory. If we consider only the effect of the O_2^0 term to order δ, then the perturbation theory prediction is that the crossing occurs at

$$\delta = 1/8C\rho \ , \tag{4.7}$$

where we have

$$C \equiv \tfrac{1}{360}x \ . \tag{4.8}$$

Equation (4.7) displays the important fact that the crossover distortion is inversely proportional to the crystal-field charge enhancement. For a very small value of ρ the distortion would have to be very large for the ground state to acquire a quadrupole moment. A very large distortion, however, would imply an extremely large elastic energy. The distortion would not be stable.

We now consider a $\langle 100 \rangle$ compression. In this case, the Γ_8 states that lower their energy with distortion, mix with the Γ_7 states. For the value of charge enhancement $\rho = 11$, used in Fig. 1, there is some mixing of these states with the Γ_7 states even for small distortions, and the ground-state energy decreases slightly. For increasing $|\delta|$, there is strong mixing, and at $|\delta| \gtrsim 4 \times 10^{-3}$ this interaction has effectively interchanged the two lowest pairs of states. The ground state now has the characteristics of a Γ_8 state with a large quadrupole moment, and the ground level now decreases linearly with distortion. Again we may use perturbation theory to approximately locate the distortion at which the large quadrupole moment is acquired. Again considering only the effect of the O_2^0 term to order δ, we find that the two levels would have crossed at a displacement

$$\delta = -1/8C\rho \ , \tag{4.9}$$

with C as defined in Eq. (4.8). The necessary size of the distortion is again inversely proportional to the charge enhancement.

The $\langle 111 \rangle$ distortions display similar behavior as shown in Fig. 2. For a $\langle 111 \rangle$ compression there is some mixing of states at very small distortion. For $|\delta| \gtrsim 2 \times 10^{-3}$, there is stronger mixing, and the ground-state energy decreases more rapidly with the linear-dependence characteristic of a state with a specific quadrupole moment. The mixing is very slight at small distortion for the $\langle 111 \rangle$ expansion. For $\delta \gtrsim 2 \times 10^{-3}$, however, the quadrupole moment appears. The quadrupole moments are induced at smaller distortions for the $\langle 111 \rangle$ case than for the $\langle 100 \rangle$. This is because the $\langle 111 \rangle$ moments are the results of a rather continuous mixing of the states. The $\langle 100 \rangle$ moments depend on level crossings and interchange of states. Also for a given distortion and ρ, the $\langle 111 \rangle$ crystal field is somewhat greater. Just as for the $\langle 100 \rangle$ case, the distortions at which the $\langle 111 \rangle$ quadrupole moments appear are inversely proportional to the charge enhancement.

Thus, the crystal field will favor a distortion beyond some minimum value for a fixed value of the enhancement factor. This minimum value depends inversely on ρ. Whether or not an equilibrium distortion occurs depends on whether or not the decrease in crystal-field energy can balance the increase in elastic energy. Therefore, increasing the probability of an equilibrium distortion requires increasing the strength of the crystal-field interaction and/or decreasing the elastic energy. Equation (4.5) suggests that a spontaneous quadrupole moment may occur if Q is, in some sense, large enough. In general, the cubic-crystal-field splitting and the elastic constants can be fixed by experiment. In the present instance

we choose to model "nonmagnetic CeBi," and therefore, choose these parameters to fit the experimental results for CeBi. The charge-enhancement factor ρ, is then treated as an adjustable parameter.

We minimize the $T=0$ free energy to determine the equilibrium distortion as a function of the charge enhancement. The resulting distortions, on varying ρ for the expansive and contractive tetragonal and trigonal distortion cases, are shown in Fig. 3. As expected, for small values of ρ the equilibrium displacement is essentially zero since the ground state remains predominantly the Γ_7. The dashed part of the curves in Fig. 3 corresponds to the range of behavior over which the ground state is acquiring a quadrupole moment either through state mixing or level crossing. [The small octupole contribution is included in these curves. This effect, together with the quadrupole formation, gives rise to the "tailing" for lower ρ values ($\rho \sim 5-10$) for the compression ($\delta < 0$) cases. At larger values of the enhancement the ground state acquires the large quadrupole moment, and the size of these distortions increases very sharply. The octupole effects are completely negligible for the $\langle 100 \rangle$ and $\langle 111 \rangle$ expansions, and there is no discernable tailing at low ρ for these cases.]

As shown in Fig. 3, at an enhancement of $\rho \geq 10$ the system can maintain a large $\langle 100 \rangle$ compression. The ground state in this case is predominately $|\pm\frac{5}{2}\rangle$ and the charge cloud is predominately oblate to the $\langle 100 \rangle$ axis. For $\rho \gtrsim 11$ a $\langle 111 \rangle$ compression or a significant $\langle 111 \rangle$, expansion is possible. For the compression mode the charge cloud is aligned predominately along the $\langle 111 \rangle$ axis, the ground state is predominately $|\pm\frac{1}{2}\rangle$. For the expansion mode the eigenstate is predominately $|\pm\frac{5}{2}\rangle$, and the charge cloud is oblate. At $\rho \gtrsim 15$, a $\langle 100 \rangle$ expansion appears. In this case the ground state is $|\pm\frac{1}{2}\rangle$ with the charge cloud aligned along the $\langle 100 \rangle$ axis. The $\langle 100 \rangle$ distortions are larger because the tetragonal elastic energy is much smaller than the trigonal elastic energy.

Figure 4 shows the zero-temperature equilibrium free energy for the four types of distortion. The $\langle 100 \rangle$ compression is most favored. Actually for a given size of distortion and a given value of the crystal-field gradient charge enhancement ρ, the $\langle 111 \rangle$ expansion mode can lower its crystal-field energy more than the $\langle 100 \rangle$ compression. However, because the tetragonal equilibrium displacement is

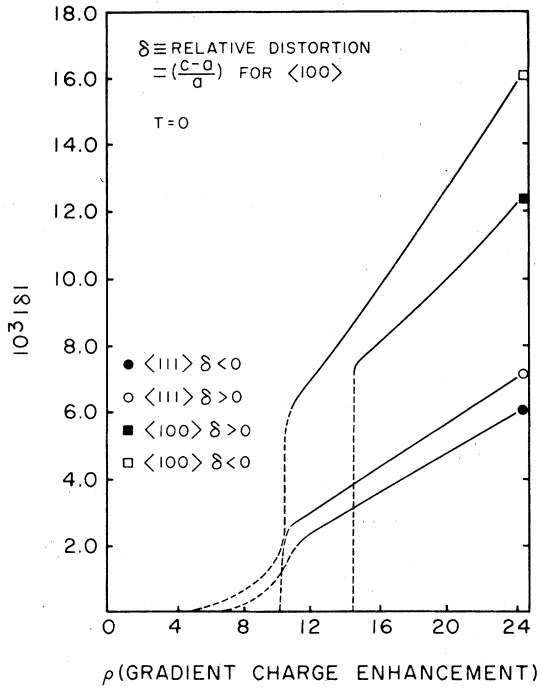

FIG. 3. Relative distortion minimizing the free energy at $T=0$ for varying crystal-field gradient charge-enhancement factor ρ. Other parameters are chosen to correspond to CeBi experimental behavior as described in text. Behavior is shown for expansive and contractive tetragonal and trigonal distortions.

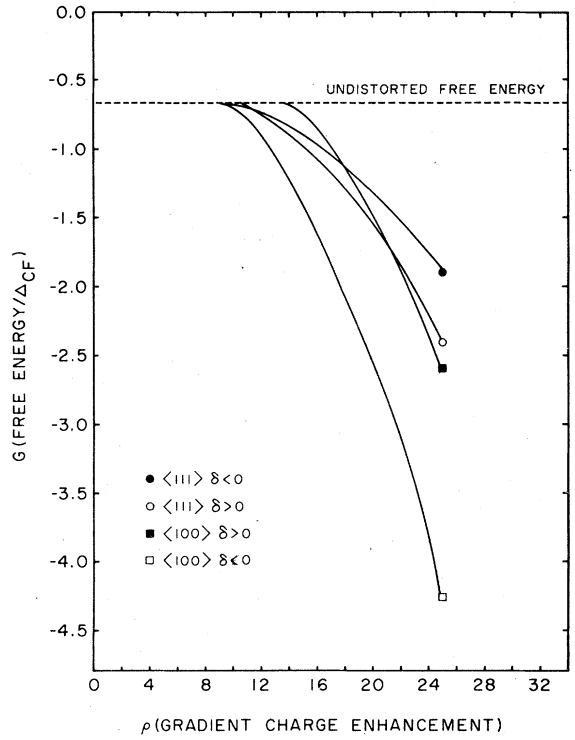

FIG. 4. Free energy at $T=0$ for varying crystal-field gradient charge-enhancement factor ρ, for each of the four types of distortion. Other parameters are chosen to correspond to CeBi experimental behavior as described in text.

larger, the ⟨100⟩ mode has the overall advantage. This importance of a lower elastic energy is also demonstrated by the behavior of the ⟨100⟩ expansion mode. The distortion is clearly at a disadvantage with respect to the crystal field. Nevertheless, at large ρ it overtakes both ⟨111⟩ modes.

The tetragonal compression for $\rho = 11$, as a function of temperature is shown in Fig. 5. We determine this curve by numerically finding the distortion which minimizes the free energy at fixed temperature. At $T = 0$ the distortion is slightly over 0.6%. It then decreases fairly rapidly to about a fourth of its initial value at a temperature $kT/\Delta_{CF} \simeq 0.65$. At this temperature the system has lost the large induced quadrupole moment. There is enough mixing of the states, however, so that a small distortion is still possible. The decrease then slows, and the curve begins to tail. Beyond $kT/\Delta_{CF} \simeq 1.0$, the tailing is due entirely to the effect of the octupole terms.

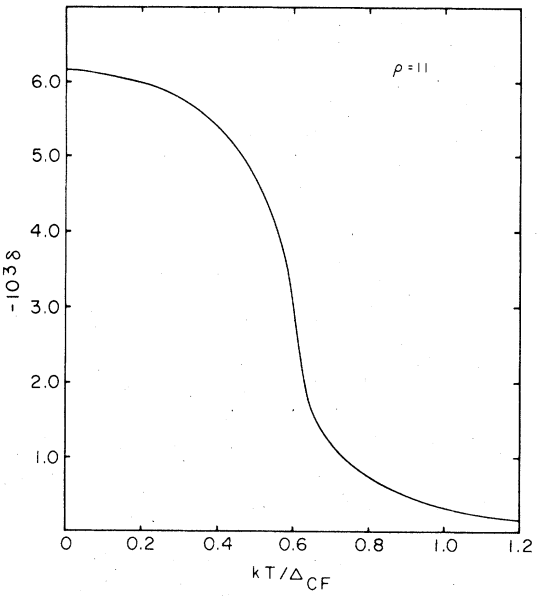

FIG. 5. Tetragonal compression, for $\rho = 11$, as a function of temperature. Other parameters are as for calculations of Fig. 3.

C. Magnetic and quadrupolar ordering, comparison with behavior in CeBi

We now consider the system with magnetic ordering. We begin by considering the behavior at $T = 0$. First, let us consider what happens in the absence of any distortion. In the strong molecular field the ground-state electronic charge cloud has the shape of a torus oblate to the direction of the field. This ground state is approximately $|\frac{5}{2}\rangle$. The charge cloud is shown in Fig. 6. To see whether we expect the

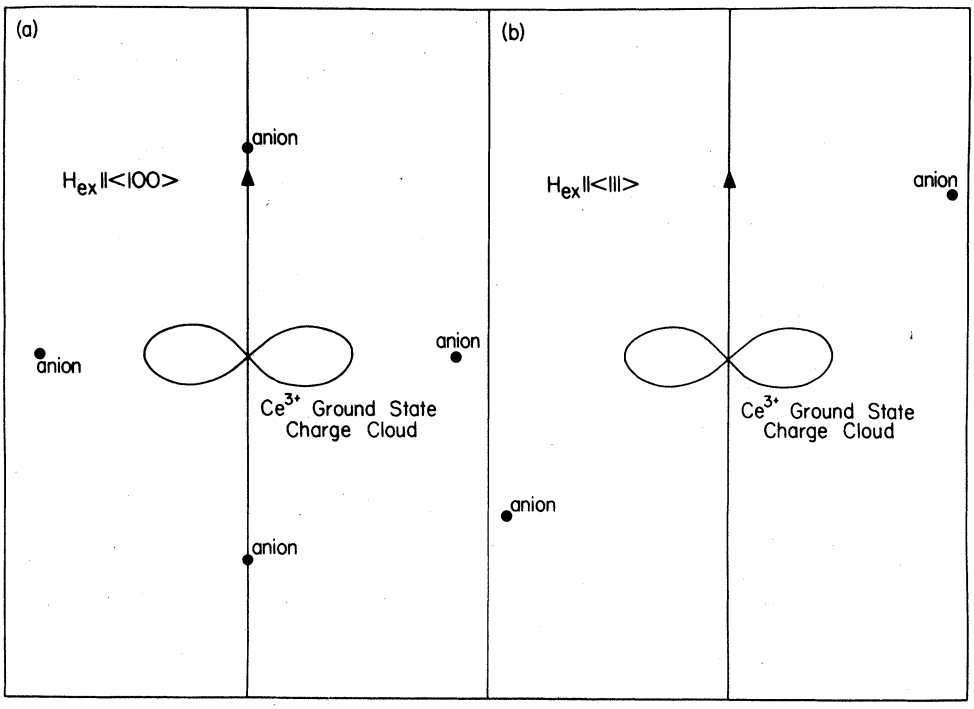

FIG. 6. Angular variation of electronic charge density in ground state of Ce^{3+} for an exchange field giving $T_N = 25$ °K. (a) Exchange field is along ⟨100⟩ and the angular dependence is shown in a (100) plane. (b) Exchange field is along ⟨111⟩, and the angular dependence is shown in a (110) plane.

easy direction of magnetization to be along ⟨100⟩ or along ⟨111⟩, we compare the ground states for those two directions of exchange field. For ordering along ⟨100⟩ the lobes of the charge cloud are directed toward the nearest-neighbor anions, resulting in strong electrostatic repulsion. For ordering along ⟨111⟩ the lobes of the cloud-charge point between the neighboring anions, and thus, experience less repulsion. The ⟨111⟩ direction is thus the preferred direction of ordering in the undistorted crystal.[9]

Now we can consider what happens when a distortion occurs in these magnetically ordered states. The magnetic ground state possess a large quadrupole moment because of the mixing of Γ_7 and Γ_8 states through the molecular field. This state, as well as the excited states, will thus react strongly to lattice distortions. The magnetically ordered state with magnetic moments along ⟨100⟩ can decrease its crystal-field energy by a tetragonal compression ($c/a < 1$). The ⟨111⟩ state can lower its energy by a trigonal expansion. This is physically expected on comparing the nature of the ground-state charge cloud to that of the excited states for each direction of magnetic alignment. In each case the ground-state charge cloud, as shown in Fig. 6, is oblate to the exchange field direction, while the excited states become increasingly prolate for increasing excitation energy. Thus, in both cases the anion motion relative to the charge clouds is such as to increase the splitting between ground and excited states. Thus, the magnetic ordering has selected from the possible tetragonal and trigonal distortion modes, a tetragonal compression in the case of ⟨100⟩ magnetic ordering and a trigonal expansion in the case of ⟨111⟩ magnetic ordering.

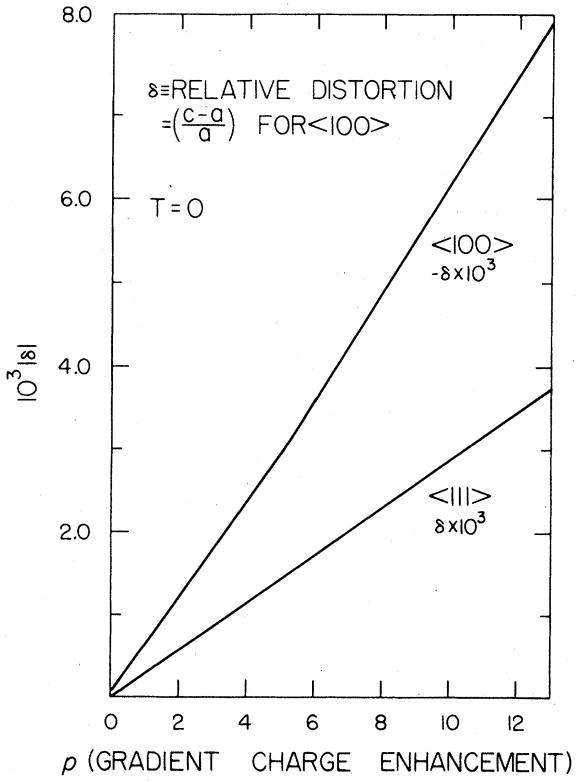

FIG. 7. Relative distortion as a function of crystal-field gradient charge-enhancement factor ρ at $T=0$. Parameters used are taken from CeBi experimental behavior as described in text.

We determine the zero-temperature equilibrium distortion for varying value of the crystal-field gradient charge-enhancement factor ρ, as shown in Fig. 7. This determination is made for equilibrium distortion along ⟨100⟩ for magnetic ordering along ⟨100⟩, and for distortion along ⟨111⟩ for magnetic ordering along ⟨111⟩, and involves minimizing the free energy with respect to magnetic moment $\langle J_z \rangle$ and distortion δ. This is done by using the usual molecular-field self-consistency requirements for each value of distortion, with a specified set of other parameters, and finding the distortion that gives an absolute minimum of the free energy. This is done with the exchange constant λ chosen to give $T_N = 25\,^\circ\mathrm{K}$ as in CeBi, and with the elastic, crystal-field, and lattice parameters chosen as previously to match the experimental behavior in CeBi.

Unlike the case of no magnetic ordering there is significant equilibrium displacement even for small ρ. This is because a quadrupole moment exists even with no distortion. For moderate values of the enhancement the magnitude of the distortion increases linearly. At higher values of ρ, the increase in size of the distortion becomes slightly faster than linear. This is in constrast to the behavior with no magnetic ordering, where the magnitude of δ varied linearly over a wide range of the enhancement. The ⟨100⟩ displacement is larger because of the smaller elastic energy. As expected from our discussion of the nonmagnetic case, the ⟨100⟩ distortion is compressive along the axis of magnetic ordering (i.e., $c/a < 1$). This is in agreement with the observed tetragonal compression with magnetic ordering of CeBi.

A comparison of the free energy for the systems with the two types of distortion as given in Fig. 7, is shown in Fig. 8. With no distortion as already discussed, the state with magnetic ordering aligned along ⟨111⟩ is more favorable. However, the fact, as shown in Fig. 7, that for a given ρ the ⟨100⟩ equilibrium distortion is always larger than the ⟨111⟩ distortion gives the ⟨100⟩ ordering an advantage with regard to lowering the crystal-field energy that becomes of increasing importance with increasing ρ. This advantage comes about because the ⟨100⟩ distortion is less disadvantageous from the point of view of increasing the elastic energy, so that the equilibrium distortion is larger. For sufficiently large ρ, this more than makes up for the fact that the crystal-field

energy goes down more quickly for increasing ⟨111⟩ expansion than for ⟨100⟩ compression. As shown in Fig. 8, the ⟨100⟩ compressive-distortion mode lowers its energy at $T=0$ very quickly for increasing ρ, and this energy crosses below the ⟨111⟩ undistorted energy at $\rho \simeq 7$, and below the ⟨111⟩ curve itself at $\rho \simeq 10$. At the crossover, the ⟨100⟩ distortion is $\delta \equiv (c-a)/a = -0.6\%$. Thus with a sufficiently large tetragonal compression, made possible by a sufficiently large enhancement of the gradient of the crystal field, the ⟨100⟩ direction becomes the easy axis of magnetic alignment.

Using the crossover value of $\rho=10$ we determine the magnetization and tetragonal distortion as a function of temperature. This is shown in Fig. 9. At zero temperature the predicted distortion is $\delta=-0.62\%$. (On going beyond the crossover value of ρ, as shown in Fig. 7, this zero-temperature value of distortion would increase approximately linearly with ρ.) The actual compression in CeBi measured by Hulliger *et al.*[6] is about 0.1%. Thus despite the crudeness of our way of parametrizing the enhancement of the crystal-field gradient, our model calculations nevertheless predict a distortion of both the type and order of magnitude observed experimentally.

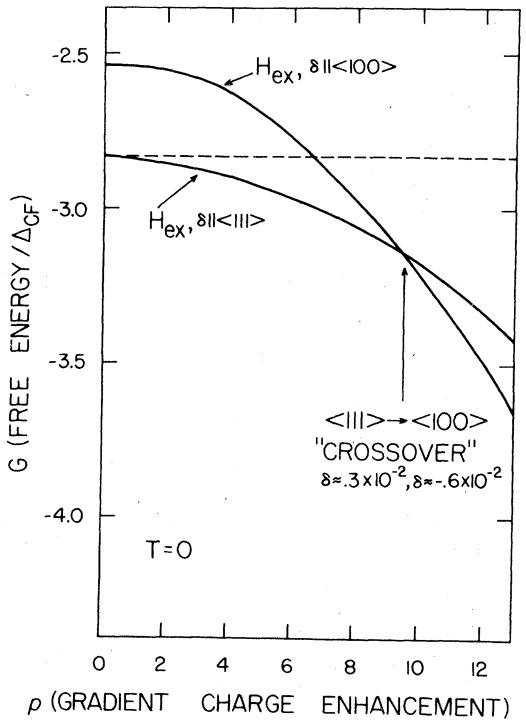

FIG. 8. Comparison of the free energy as a function of ρ for the two directions of magnetic ordering. For a specified ρ, this gives the free energy corresponding to the displacement shown in Fig. 7.

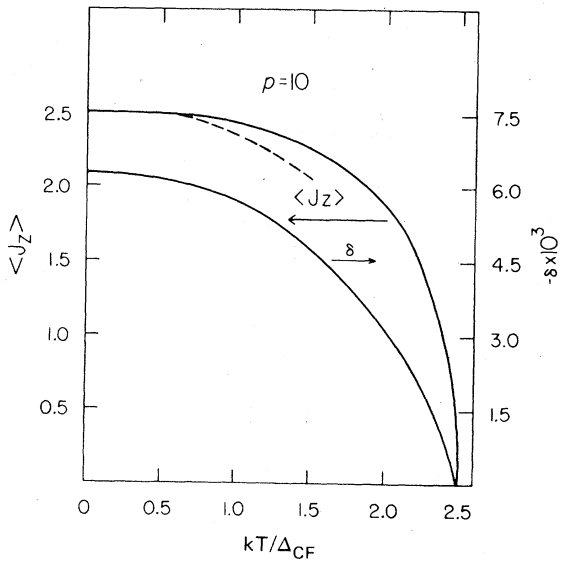

FIG. 9. Magnetization and tetragonal distortion with varying temperature for $\rho=10$. Other parameters are as in Fig. 7 and 8. For purposes of comparison, the low-temperature part of the magnetization curve corresponding to the Brillouin function for $J=\frac{5}{2}$ is shown as a dashed curve.

The magnetization in Fig. 9 is relatively flat at low temperatures, i.e., compared to the magnetization behavior corresponding to the Brillouin function for $J=\frac{5}{2}$. This flatness of the magnetization comes about through the wave-function mixing associated with the distortional (quadrupolar) effects. For sufficiently large ρ, even in the absence of magnetic ordering these effects tend to give a ground-state doublet that is predominantly $|\pm\frac{5}{2}\rangle$. So even a small molecular field will split the doublet and create a new ground state with a moment close to saturation. Thus the quadrupolar ordering acts to reinforce the molecular field in maintaining the magnetic moment. The degree of flatness varies markedly with ρ. For a smaller ρ, even say $\rho=7$, the flatness of the magnetization curve (relative to that for the magnetization corresponding to the Brillouin function with $J=\frac{5}{2}$) would largely disappear, while for a large ρ, say $\rho=15$, the magnetization is essentially flat up to half the Néel temperature. (This marked variation with ρ corresponds to the existence of spontaneous quadrupolar ordering, in the absence of magnetic ordering, for $\rho \gtrsim 10$ as discussed in Sec. IV B above.) This large induced quadrupolar effect, associated with substantial crystal-field gradient enhancement, may be the physical mechanism responsible for the experimental result observed by Cable and Koehler[2] that the sublattice magnetization in CeBi remains close to saturation over a temperature range close to $\frac{2}{3}$ of the way to the Néel temperature.

Thus, in summary, we see that our simple model for the crystal-field gradient charge enhancement allows us to understand the occurence of strong ⟨100⟩ magnetic anisotropy in CeBi and CeSb in association with a compressive ($c/a < 1$) tetragonal distortion. The order of magnitude of tetragonal distortion observed[6] and its compressive nature are in agreement with the expectation from our calculations. The very flat sublattice-magnetization curve for increasing temperature[2] can also be understood as a consequence of the crystal-field gradient enhancement.

The key parameter in the present theory is ρ, the crystal-field gradient charge-enhancement factor. The key result associated with the behavior of that parameter is the existence of a threshold value of ρ, dependent on material parameters, for a sharp changeover from trigonal distortion and ⟨111⟩ magnetic anisotropy to tetragonal distortion and ⟨100⟩ anisotropy. The limited experimental information, inferred from the crystal-field variation between the cerium monopnictides as discussed in Sec. II, leads us to expect a value of ρ for CeBi beyond the threshold for that material, and having such a value would then explain the experimental behavior of CeBi. Presumably a similar picture holds for CeSb. At present, however, there is no direct measurement of ρ.

A particularly valuable type of experiment would involve the application of a uniaxial stress in conjunction with magnetization or neutron scattering experiments. With such experiments one could measure ρ directly. By applying a stress, one can vary c/a and measure the crystal-field splitting with neutron scattering. Alternatively one can dilute the Ce in CeBi or CeSb with La and/or Y. For sufficient dilution the material becomes paramagnetic, but the crystal field is probably little changed from that in the pure compound. [For example,[3] in $Ce_x(La_{0.76}Y_{0.24})_{1-x}Sb$ or $Ce_x(La_{0.76}Y_{0.24})_{1-x}Bi$, the average lattice constant does not vary with x. Then high-field anisotropic magnetization or susceptibility measurements[3,9] could be used to determine the crystal-field splitting and its variation with c/a under stress.

ACKNOWLEDGMENT

This research was supported in part by NSF Grant No. DMR 77-06721.

[1]T. Tsuchida and W. E. Wallace, J. Chem. Phys. 43, 2087 (1965).
[2]J. W. Cable and W. C. Koehler, AIP Conf. Proc. 5, *Magnetism and Magnetic Materials - 1971,* 1381 (1972).
[3]B. R. Cooper, M. Landolt, and O. Vogt, *Proceedings International Conference on Magnetism ICM - 73,* (Publishing House Nauka, Moscow, 1974) Vol. 5, p. 354.
[4]H. Bartholin, D. Florence, W. Tcheng-si, and O. Vogt, Phys. Status Solidi A 24, 631 (1974).
[5]G. H. Lander, M. H. Mueller, and O. Vogt, AIP Conf. Proc. 24, *Magnetism and Magnetic Materials - 1974,* 430 (1975).
[6]F. Hulliger, M. Landolt, H. R. Ott and R. Schmelczer, J. Low Temp. Phys. 20, 269 (1975).
[7]T. Tsuchida and W. E. Wallace, J. Chem. Phys. 43, 2885 (1965).
[8]G. Busch and O. Vogt, Phys. Lett. 20, 152 (1966); G. Busch and O. Vogt, Phys. Lett. A 25, 449 (1967).
[9]B. R. Cooper and O. Vogt, J. Phys. (Paris) 32, C1 (1971).
[10]B. R. Cooper, A. Furrer, W. Buhrer, and O. Vogt, Solid State Commun. 11, 21 (1972).
[11]H. Bartholin, D. Florence, W. Tcheng-Si, and O. Vogt, Phys. Status Solidi A 29, 275 (1975).
[12]J. Rossat-Mignod, P. Burlet, J. Villain, H. Bartholin, W. Tcheng-Si, and D. Florence, Phys. Rev. B 16, 440 (1977).
[13]P. Fischer, B. Lebech, G. Meier, B. D. Rainford, and O. Vogt, J. Phys. C 11, 345 (1978).
[14]G. Meier, P. Fischer, W. Halg, B. Lebech, B. D. Rainford, and O. Vogt, J. Phys. C 11, 1173 (1978).
[15]B. R. Cooper, in *Magnetism in Metals and Metallic Compounds,* edited by J. T. Lopuszanski, A. Pekalski, and J. Przystawa (Plenum, New York, 1976), p. 225.
[16]B. R. Cooper, *Proceedings of the Second International Conference on the Electronic Structure of the Actinides,* edited by J. Mulak, W. Suski, and R. Troc (Zaklad Narodwy, Ossolinskich, Wroclaw, Poland, 1976), p. 369.
[17]R. J. Birgeneau, E. Bucher, J. P. Maita, L. Passell, and K. C. Turberfield, Phys. Rev. B 8, 5345 (1973).
[18]A brief preliminary report was given in R. Siemann and B. R. Cooper, Bull. Am. Phys. Soc. 23, 401 (1978).
[19]B. R. Cooper, Phys. Rev. B 17, 293 (1978).
[20]A. Furrer, W. Buhrer, H. Heer, W. Halg, J. Benes, and O. Vogt, *Neutron Inelastic Scattering 1972,* (International Atomic Energy Authority, Vienna, 1972), p. 563.
[21]H. Heer, A. Furrer, and W. Halg, J. Magn. Magn. Mater. 3, 55 (1976).
[22]H. Heer, A. Furrer, and W. Halg, in *Crystal Field Effects in Metals and Alloys,* edited by A. Furrer (Plenum, New York, 1977), p. 278.
[23]H. Bartholin, D. Florence, G. Parisot, J. Paureau, and O. Vogt, Phys. Lett. A 60, 47 (1977).
[24]M. T. Hutchings, in *Solid State Physics,* edited by F. Seitz and D. Turnbull (Academic, New York, 1964), Vol. 16, p. 227.
[25]K. W. H. Stevens, Proc. Phys. Soc. London A 65, 209 (1952).
[26]A. J. Freeman and R. E. Watson, Phys. Rev. 127, 2059 (1962).
[27]Y. L. Wang and B. R. Cooper, Phys. Rev. 172, 539 (1968).
[28]J. DeLaunay, in *Solid State Physics,* edited by F. Seitz and D. Turnbull, (Academic, New York, 1956), Vol. 2, p. 219.
[29]B. Luthi, P. S. Wang, and E. Bucher, *Proceedings of the First International Conference on Crystalline Electric Field Effects in Metals and Alloys, Montreal (1974),* p. 272.
[30]P. Bak and P. A. Lindgard, J. Phys. C 6, 3774 (1973).